DOI 10.1007/s11204-021-09701-7
Soil Mechanics and Foundation Engineering, Vol. 58, No. 1, March, 2021 (Russian Original No. 1, January-February, 2021)

SOIL MECHANICS

A VISCOELASTIC-PLASTIC CONSTITUTIVE MODEL OF CREEP IN CLAY BASED ON IMPROVED NONLINEAR ELEMENTS

UDC 624.131.5

Peng Ren,[1,3] Peng Wang,[1,2*] Yin Tang,1 Zi-dong Zhang[1]
[1]Sichuan Institute of Building Research, Chengdu, China; [2]Sichuan Construction Engineering Quality Testing Center, State Key Laboratory of Geohazard Prevention and Geoenvironment Protection, Chengdu, China; [3]Chengdu University of Technology, Chengdu; China.
*Corresponding author Email: wrpyscre@163.com.

A Triaxial creep experiment was performed with Chengdu clay. The results demonstrate that the deformation of clay includes instantaneous elastic strain, attenuated creep deformation, steady creep deformation, and accelerated creep deformation. In view of the nonlinear properties of creep, an improved nonlinear viscous element describing attenuating creep and an improved fractional order viscous element describing accelerating creep are established, and a one-dimensional nonlinear fractional order five-element creep model is developed with the two improved elements. The model can theoretically describe the entire process of creep. The nonlinear fractional order five-element model and the traditional five-element model were employed to verify the creep test. Compared with the traditional five-element creep model, the nonlinear fractional order creep model more faithfully reproduces the experimental data and more accurately describes the deformation trend in each stage, especially the accelerated creep stage.

Introduction

Clay creep refers to the deformation of clay under stress over time. Understanding and predicting creep behavior is important for quantifying the stability of clay for engineering purposes [1-3]. At present, a major goal is to establish a constitutive model with clear physical significance, strong reproducibility, few parameters, and simple form which accurately reflects the entire clay creep process [4-6]. Such a model would include an empirical term, viscoelastic term [7], viscoplastic term [8], and viscoelastic-plastic term [9].

Numerous studies have shown that clay deformation has significant nonlinear properties with increasing stress and longer timescales, especially under high-stress conditions [10]. The element model has the advantages of clear physical significance and few parameters and has been widely studied and applied. However, it has been found that the traditional element model can only reflect the creep attenuation stage and has difficulty describing the acceleration stage. To address this, three methods have been used to describe the nonlinear components of clay creep. The first method establishes the strain-time and strain-stress relationships empirically to define a nonlinear creep model [11]. This model can accurately reflect the clay creep properties but has some disadvantages such as a limited range and lack of a theoretical basis. The second method establishes a nonlinear creep model by integrating one or several nonlinear parameters to replace the linear parameters [12]; however, this approach does not adequately reflect the effect of stress or time on creep. The third method generates

Translated from Osnovaniya, Fundamenty i Mekhanika Gruntov, No. 1, p. 7, January-February, 2021.

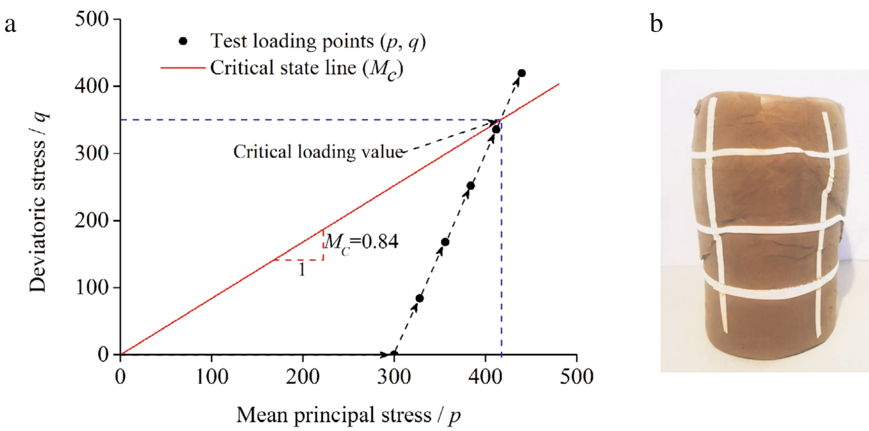

Fig. 1. Stress path of the creep test in the p–q plane (a) and test failure sample (b).

a nonlinear creep model with fractional order calculus theory [13], which produces a complex form that is difficult to calculate.

In this paper, the results of a creep experiment on Chengdu clay are employed to establish improved nonlinear viscous and fractional viscous elements and develop a nonlinear creep model. The parameters of the resulting nonlinear fractional order five-element model are discussed and analyzed. By comparing with the traditional five-element creep model, the robustness of the new model is verified.

Material and Test Instruments

The clay was taken from the Yulong Mountains, Chengdu. The specimen is pale yellow with gray and white calcareous nodules, with no obvious cracks and a hard plasticity. The basic mechanical properties of the clay are: ρ_d = 1.63 g/cm^3, w = 22.3%; w_L = 46.1%; w_P = 19.5%; c = 57.1 kPa; φ = 16.8°. A css-2901ts soil triaxial rheological testing machine (Changchun Testing Machine Institute, Jilin, China) was employed for the creep experiment.

The creep test procedure is as follows:

(1) Sample preparation. The samples were classified in accordance with their natural moisture content and dry density of the clay and were saturated in a vacuum chamber for two days.

(2) Sample installation. The sample is 78 mm in height and 39 mm in diameter. The samples were loaded onto the experimental apparatus with as little disturbance as possible, and an initial pressure of 2 kPa was applied along the axis.

(3) Sample consolidation. The confining pressure was then set to increase to 300 kPa at a rate of 0.5 kPa per minute. This consolidated the samples, assuming that pore water pressure dissipated by > 95%.

(5) Sample loading. The total deviatoric stress was 524.45 kPa. In the experiment design, the total stress is subdivided into five grades, and the load increment of each grade is given by $\Delta q = kq_f/x$, where k is the material strength reduction factor (0.65-0.85), q_f is the failure deviatoric stress, and x is the stage number with a loading rate of 0.1 kPa per minute. The loading stress path of the sample in the p–q plane is shown in Fig. 1a.

(6) Test stability standard. The stability standard of the experiments is axial deformation < 0.01 mm/day. A failed sample is shown in Fig. 1b.

Creep Testing Results

From the results of the experiment, the creep-time history curve can be obtained (Fig. 2).

After each stage of loading, the strain on the clay increases rapidly, indicating that clay deformation includes instantaneous strain. The strain also increases with time, indicating a creep deformation

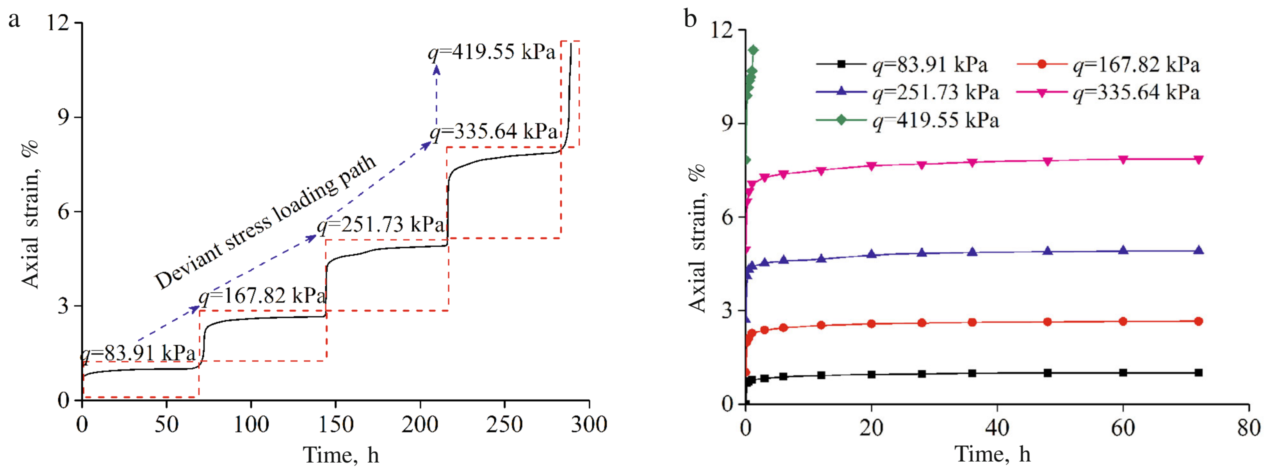

Fig. 2. Time curve of clay creep: a) whole-loading; b) grading loading.

component. Additionally, with increasing loading stress, the corresponding instantaneous deformation and creep deformation also increase.

Under a low stress condition, the creep rate of clay gradually attenuated to 0, and creep deformation converged. This result indicates that creep deformation attenuates. Under high stress conditions, the creep rate of clay is constant or increases, and creep deformation increases until sample failure. This indicates that clay creep deformation includes a component of steady or accelerated creep deformation.

At the instant deformation stage of clay, the relationship between deformation and loading time is linear. However, in either the steady creep stage or accelerated creep stage, the relationship between deformation and loading time is nonlinear.

Clay Nonlinear Constitutive Model

Improved nonlinear viscous element

Xiong and Zhao [14-15] concluded that the viscosity coefficient of rock and soil is negatively related to the loading time. The nonlinear viscosity coefficient function of the negative power relation is given as:

$$\eta(t) = \eta_0 (t/t_0)^{-\lambda_1}, \tag{1}$$

where t is time, t_0 is unit time and its value is 1, $\eta(t)$ is the viscosity coefficient at time t, η_0 is the initial viscosity coefficient, and λ_1 is the nonlinear parameter of clay.

The derivative of Eq. (1) with respect to time is

$$d\eta(t)/dt = -\eta_0 \lambda_1 (t/t_0)^{-\lambda_1 - 1}. \tag{2}$$

When $\lambda_1 > 0$ and $d\eta(t)dt < 0$, the viscosity decreases with time, and the mechanical properties of the clay show a nonlinear softening. When $\lambda_1 < 0$ and $d\eta(t)dt > 0$, the viscosity coefficient increases with time, and the mechanical properties of the clay show a nonlinear hardening. The nonlinear viscosity coefficient can thus reflect the creep propensity of clay through different values of λ_1.

Improved fractional order viscous element

Fractional calculus theory has a rigorous derivation process and a sound theoretical basis, especially for the memory effect of the loading history of materials, and it is widely used in the development of various constitutive models [16-17]. In constitutive models, fractional calculus often adopts the

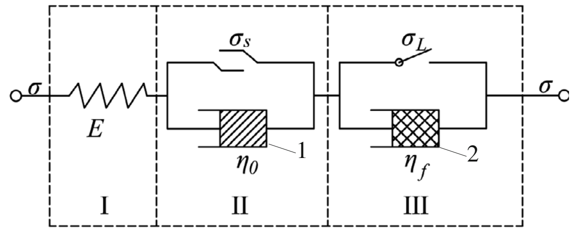

Fig. 3. Nonlinear fractional order five-elements creep model: 1) nonlinear viscosity element and 2) improved fractional viscous component.

Riemann-Liouville theory [18-19]. The mathematical function f is hypothetically continuously integrable over $(0, +\infty)$, and for $t > 0$ and $\mathrm{Re}(n) \geq 0$, the corresponding fractional integral is

$$\frac{d^{-n}[f(t)]}{dt^{-n}} = {}_{t_0}D_t^{-n} f(t) = \frac{1}{\Gamma(n)}\int_{t_0}^{t} (t-\xi)^{n-1} f(\xi)d\xi, \tag{3}$$

where $\Gamma(n)$ is the gamma function, and n is the fractional order.

If $f(t)$ is integrable in the vicinity of $t = 0$, and $n \geq 0$, the Laplace transformation $f(t)$ of fractional order calculus is

$$\left.\begin{aligned} L\left[{}_0D_t^{-n} f(t), p\right] &= p^{-n}\overline{f}(p) \\ L\left[{}_0D_t^{n} f(t), p\right] &= p^{n}\overline{f}(p) \end{aligned}\right\}. \tag{4}$$

Using fractional order calculus theory and nonlinear viscous elements, a new kind of fractional order viscous element is developed to describe the accelerated clay creep stage. The constitutive model is given by

$$\sigma(t) = \eta_f \left(\frac{t}{t_0}\right)^{-\lambda_2} \frac{d^n \varepsilon(t)}{dt^n}, \tag{5}$$

where η_f is the initial viscosity coefficient of the fractional order viscous elements, and λ_2 is a material parameter. If $n = 0$, the element is elastic and can be described by the properties of an ideal solid; if $n = 1$, the element obeys Newtonian viscosity and can be described by the properties of an ideal fluid.

When $\sigma(t)$ is constant, the fractional integration of Eq. (5) yields

$$\varepsilon(t) = \frac{\sigma}{\eta_f} \frac{\Gamma(\lambda_2 + 1)}{\Gamma(n + \lambda_2 + 1)} \left(\frac{t}{t_0}\right)^{(n+\lambda_2)}. \tag{6}$$

The derivative of Eq. (6) with respect to time gives

$$\dot{\varepsilon}(t) = \frac{\sigma}{\eta_f} \frac{\Gamma(\lambda_2 + 1)(n + \lambda_2)}{\Gamma(n + \lambda_2 + 1)} \left(\frac{t}{t_0}\right)^{(n+\lambda_2-1)}. \tag{7}$$

When $n + \lambda_2 > -1$ and $\varepsilon(t) > 0$, the improved fractional order viscous element describes the accelerated creep of clay.

The nonlinear creep element of clay

The deformation properties of clay under the influence of stress over time are extremely complicated. To describe this process, a five-element constitutive model is constructed with elastic, nonlinear viscous, improved fractional viscous, plasticity, and switch elements, as shown in Fig. 3. In Fig. 3, part I is an elastomer composed of an elastic element that describes the instantaneous elastic strain. Part II is an improved nonlinear viscoplastic body comprising a nonlinear viscous element and a plastic element in parallel, which describes the attenuation creep and steady creep. Part III is a nonlinear fractional order body composed of an improved fractional viscous element and switching element, which describes accelerated creep.

For the nonlinear five-element creep model, when t = 0 and under a constant stress σ, the relationship between the stress and strain of the model is given as

$$\begin{cases} \varepsilon = \varepsilon_{\mathrm{I}} + \varepsilon_{\mathrm{II}} + \varepsilon_{\mathrm{III}} \\ \sigma = \sigma_{\mathrm{I}} = \sigma_{\mathrm{II}} = \sigma_{\mathrm{III}} \end{cases}, \tag{8}$$

where σ, σ_{I}, σ_{II}, and σ_{III} are the total stress and the stress in parts I, II, III, respectively, and ε, ε_{I}, $\varepsilon_{\mathrm{II}}$, and $\varepsilon_{\mathrm{III}}$ are total strain and the strain in parts I, II, and III, respectively.

The elastomer constitutive model of part I is given by

$$\varepsilon_{\mathrm{I}} = \frac{\sigma_{\mathrm{I}}}{E_0} = \frac{\sigma}{E_0}, \tag{9}$$

where E_0 is the elastic modulus of the elastomer.

The nonlinear viscoplastic body element of part II is given by

$$\sigma_{\mathrm{II}} = \eta_0 \left(\frac{t}{t_0}\right)^{-\lambda_1} \dot{\varepsilon}_{\mathrm{II}}. \tag{10}$$

Separating variable integrals from Eq. (10) gives

$$\varepsilon_{\mathrm{II}} = \frac{\langle \sigma - \sigma_s \rangle}{\eta_0} \frac{1}{1+\lambda_1} \left(\frac{t}{t_0}\right)^{1+\lambda_1}, \tag{11}$$

where σ_s is the yield stress; $\langle \sigma - \sigma_s \rangle = 0$ when $\sigma \le \sigma_s$, and $\langle \sigma - \sigma_s \rangle = \sigma - \sigma_s$ when $\sigma > \sigma_s$.

For the nonlinear fractional body element of part III, the stress relationship of the viscoplastic body is given by

$$\langle \sigma - \sigma_L \rangle = \begin{cases} 0 & \sigma \le \sigma_L \\ \sigma - \sigma_L & \sigma > \sigma_L \end{cases}, \tag{12}$$

where σ_L is the long-term strength of the clay.

Therefore, according to Eqs. (6) and (12), the relationship of a nonlinear fractional body can be obtained:

$$\varepsilon_{\mathrm{III}} = \frac{\langle \sigma - \sigma_L \rangle}{\eta_f} \frac{\Gamma(\lambda_2 + 1)}{\Gamma(n + \lambda_2 + 1)} \left(\frac{t}{t_0}\right)^{(n+\lambda_2)}. \tag{13}$$

In sum, according to Eqs. (8), (9), (11), and (13) and given an initial strain ε_0, the nonlinear fractional order five-element model of creep is given by

$$\varepsilon = \varepsilon_0 + \frac{\sigma}{E_0} + \frac{\langle \sigma - \sigma_s \rangle}{\eta_0} \frac{1}{1+\lambda_1} \left(\frac{t}{t_0}\right)^{1+\lambda_1} + \frac{\langle \sigma - \sigma_L \rangle}{\eta_f} \frac{\Gamma(\lambda_2 + 1)}{\Gamma(n + \lambda_2 + 1)} \left(\frac{t}{t_0}\right)^{(n+\lambda_2)}. \tag{14}$$

When λ_1 = 0 and λ_2 = 0,

$$\varepsilon = \varepsilon_0 + \frac{\sigma}{E_0} + \frac{\langle \sigma - \sigma_s \rangle}{\eta_0} \frac{t}{t_0} + \frac{\langle \sigma - \sigma_L \rangle}{\eta_f} \frac{1}{\Gamma(n+1)} \left(\frac{t}{t_0}\right)^{n}. \tag{15}$$

Equation (15) represents the constitutive model composed of the traditional element model and fractional components in series. This model describes linear creep deformation, which demonstrates that the conventional linear creep model is a special case of this model.

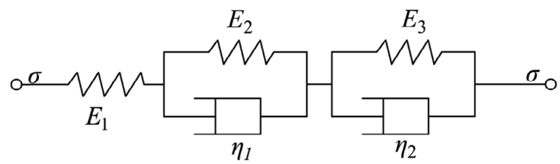

Fig. 4. Traditional five-elements creep model.

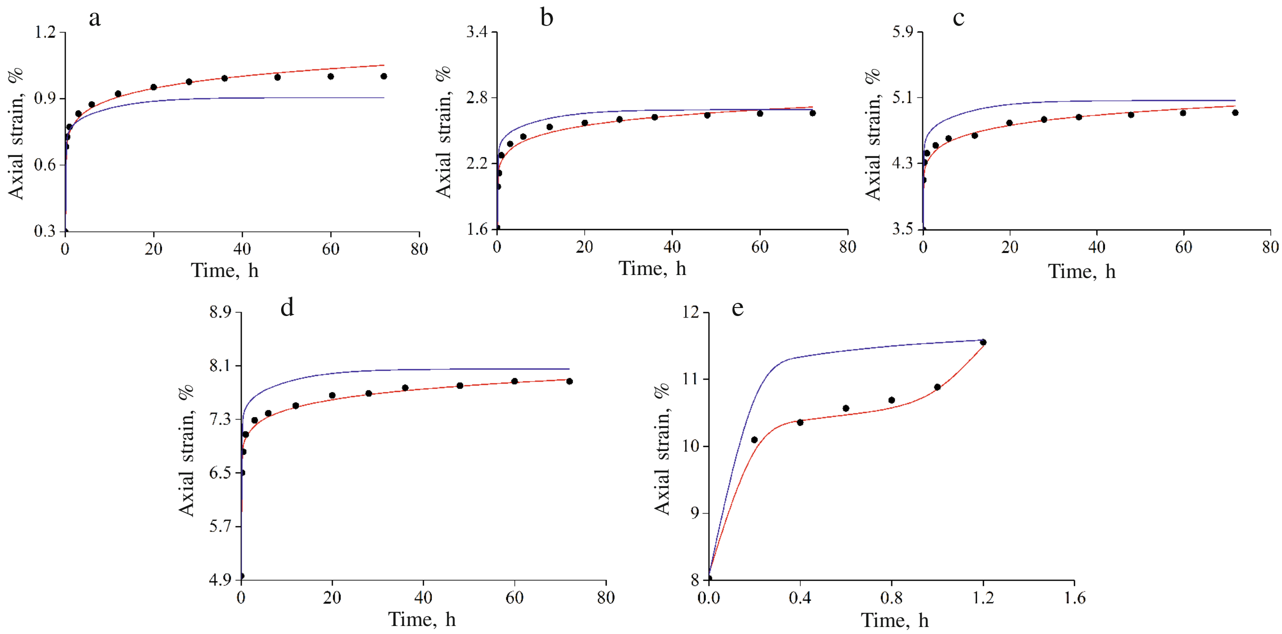

Fig. 5. Comparison of the creep model calculations and experimental data (●):
a) q = 83.91 kPa; b) q = 167.82 kPa; c) q = 251.73 kPa; d) q = 335.64 kPa; e) q = 419.55 kPa;
——) nonlinear fractional order model and ——) traditional five-element model.

When $\sigma - \sigma_L \leq 0$, Eq. (16) can be obtained from Eq. (14):

$$\varepsilon(t) = \varepsilon_0 + \frac{\sigma}{E_0} + \frac{\langle \sigma - \sigma_s \rangle}{\eta_0} \frac{1}{1+\lambda_1} \left(\frac{t}{t_0} \right)^{1+\lambda_1} . \tag{16}$$

If $-1 < \lambda_1 < 0$, clay strain gradually converges over time, and the model describes decay creep. If $\lambda_1 = 0$, the clay strain increases at a constant rate, and the model describes steady creep.

When $\sigma - \sigma_L > 0$, if $\lambda_2 > 0$ and $\lambda_1 > -1$, the strain increases rapidly. This behavior demonstrates that the model can describe the accelerated creep stage.

Through different values of λ_1 and λ_2 the nonlinear fractional constitutive model established here can theoretically describe the entire process of clay creep.

Identification of the Creep Model

At present, common methods for evaluating constitutive models include the peak point partial derivative method and the curve fitting method [20]. To verify the validity of the nonlinear fractional order five-element creep model (E_0 = 60 MPa, λ_1 = –0.90, η_0 = 522 MPa·h, λ_2 = 5.1, η_f = 0.6 MPa·h, and n = 3.0) presented in this paper and the traditional five-element creep model (E_1 = 55 MPa, E_2 = 60 MPa, E_3 = 80 MPa, η_1 = 530 MPa·h, and η_2 = 407 MPa·h) (Fig. 4) are employed to fit the curve of the creep test data. The deformation values calculated by the two creep models are obtained, and the calculated results are compared with the creep test data for verification, as shown in Fig. 5.

The traditional five-element creep model is as follows:

$$\varepsilon_{\mathrm{T}}=\sigma_{\mathrm{T}}\left[\frac{1}{E_1}+\frac{1-e^{\left(-E_2 t/\eta_1\right)}}{E_2}+\frac{1-e^{\left(-E_3 t/\eta_2\right)}}{E_3}\right], \tag{17}$$

where ε_{T} and σ_{T} are the strain and stress of creep, respectively; E_1, E_2, and E_3 are the elastic models of the elastic elements; and η_1 and η_2 are the viscosity coefficients of the viscous elements.

The data in Fig. 5 demonstrate that the calculated values of the nonlinear fractional order creep model are in good agreement with the creep test values, and the deformation trends of the calculated values and the experimental values at each creep stage are highly consistent. In addition, the nonlinear fractional order creep model more accurately reflects the creep properties of clay. Moreover, the traditional five-element creep model poorly reflects the creep property of clay. In the attenuated creep and steady creep stages, the calculated value of the traditional five-element model is roughly consistent with the experimental value. During the accelerated creep stage, however, the calculated values of the model are completely inconsistent with the experimental value. Therefore, compared with the traditional five-element creep model, the nonlinear fractional creep model can more accurately describe the entire process of clay creep, demonstrating the robustness of the model.

Conclusions

We performed a triaxial creep experiment and developed a nonlinear fractional five-element creep model. Two creep models are employed to fit the experimental data for comparison. The nonlinear fractional creep model is shown to be robust, and the following conclusions are obtained:

(1) A triaxial creep experiment demonstrated that clay deformation includes instantaneous elastic deformation, attenuation creep deformation, steady creep deformation, and accelerated creep deformation. The clay creep exhibits significant nonlinearity in each stage.

(2) The improved nonlinear viscous element and the improved fractional viscous element are each constructed with an attenuation exponential function. The nonlinear fractional order five-element creep model for clay is established with two improved nonlinear elements.

(3) By analyzing the influence of parameters λ_1 and λ_2 on the model, it is found that the nonlinear fractional order creep model can describe the various stages of clay creep by employing different values of λ_1 and λ_2.

(4) By comparing the two creep models, we demonstrate that the calculated value of the nonlinear fractional order five-element model more faithfully reproduces the experimental values. In addition, the model more accurately describes the deformation trend in each stage, especially in the accelerated creep stage. Thus, the model developed here can accurately describe the entire process of clay creep.

Acknowledgments

We acknowledge the strong support provided by the following: Geotechnical Engineering Institute, Sichuan Institute of Building Research; State Key Laboratory of Geohazard Prevention and Geoenvironment Protection; Chengdu University. This work was supported by Sichuan Science and Technology Program (No. 2019YJ0551) and Sichuan Huaxi Group Co., Ltd. (No. HXKX20181030). Peng Ren and Peng Wang contributed equally to this work. We thank Edanz Editing China for editing the English text of a draft of this manuscript.

REFERENCES

1. B. G. Sexton, B. A. McCabe, M. Karstunen, and N. Sivasithamparam, "Stone column settlement performance in structured anisotropic clays: the influence of creep," *J. Rock Mech. Geotech. Eng.*, **8**(5), 672-688 (2016).

2. P. J. Venda Oliveira, A.A.S. Correia, and L.J.L. Lemos, "Numerical prediction of the creep behaviour of an unstabilised and a chemically stabilised soft soil," *Comput. Geotech.*, **87**, 20-31 (2017).
3. C. Ma, T. Zhang, and W. Yao, "An assessment of the osmotic pressure effect on the creep properties of silty mudstone," *Soil Mech. Found. Eng.*, **56**, 314-320 (2019).
4. M. Leoni, M. Karstunen, and P. A. Vermeer, "Anisotropic creep model for soft soils," *Geotechnique*, **58**, 215-226 (2008).
5. Z. Y. Yin, Q.-Y. Zhu, and D. M. Zhang, "Comparison of two creep degradation modeling approaches for soft structured soils," *Acta Geotech*, **12**, 1395-1413 (2017).
6. M. Kavvadas and A. Kalos, "A time-dependent plasticity model for structured soils (TMS) simulating drained tertiary creep," *Comput. Geotech.*, **109**(5), 130-143 (2019).
7. K. F. Li, R. Li, C. L. Qiu, and R. J. Tan, "Consolidated drained creep model of soft clay in Tianjin coastal areas," *Proceedings of GeoShanghai 2018 International Conference*: Fundamentals of Soil Behaviours 2018 Shanghai, Elasticer, Singapore, 157-165.
8. C. Yang, J. P. Carter, D. Sheng, and S. W. Sloan, "An isotach elastoplastic constitutive model for natural soft clays," *Comput. Geotech.*, **77**, 134-155 (2016).
9. W. H. Zhou, F. Tan, and K. V. Yuen, "Model updating and uncertainty analysis for creep behavior of soft soil," *Comput. Geotech.*, **100**, 135-143 (2018).
10. S. R. Lo, M. R. K, and C. T. Gnanendran, "Consolidation and creep settlement of embankment on soft clay: prediction versus observation," *Geotechnical Predictions and Practice in Dealing with Geohazards*, **25**, 77-94 (2013).
11. J. G. Zhu and J.-H. Yin, "Drained creep behavior of soft Hong Kong marine deposits," *Geotechnique*, **51**, 471-474 (2001).
12. Y. F. Jin, Z. Y. Yin, W. H. Zhou, J. H. Yin, and J. F. Shao, "A single-objective EPR based model for creep index of soft clays considering L2 regularization," *Eng. Geol.*, **248**, 242-255 (2019).
13. M. Liao, Y. Lai, E. Liu, and X. Wan, "A fractional order creep constitutive model of warm frozen silt," *Acta Geotech.*, **12**, 377-389 (2016).
14. Y. Zhao, P. Cao, Y. Wen, Y. Wang, and H. Chai, "Elastovisco-plastic rheological experiment and nonlinear rheological model of rocks," *Chin. J. Rock Mech. Eng.*, **27**, 477-486 (2008).
15. L. Xiong, L. Yang, and Y. Zhang, "Composite viscoelasto-plastic rheological model for hard rock," *J. Central South Univ. (Sci. Technol.)*, **38**, 188-193 (2010).
16. L. Chen, S. G. Chen, H. Zhang, and J. S. Yang, "A nonlinear viscoelasto-plastic creep model based on fractional calculus," *J. Sichuan Univ.*, **45**, 7-11 (2013).
17. R. Li, J. Yue, S. Feng, H. Luo, and T. Wang, "Improved fractional order derivative empirical power function model for describing the creep of asphalt mortar," *J. Build. Mater.*, **18**(2), 237-242 (2015).
18. R. C. Koeller, "Application of fractional calculus to the theory of viscoelasticity," *J. Appl. Mech.*, **51**(2), 229-307 (1984).
19. K. Adolfsson, M. Enelund, and P. Olsson, "On the fractional order model of viscoelasticity," *Mech. Time-Depend. Mater.*, **9**(1), 15-34 (2005).
20. J. Zhu, H. Cheng, and Y. Yao, "Statistical damage softening model of fractured rock based on SMP failure criterion and its application," *Chin. J. Rock Mech. Eng.*, **32**, 3160-3168(2013).